Vol. 13, No. 2 (2025), pp.108–132

CHITKARA UNIVERSITY

Journal of Pharmaceutical Technology Research and Management

Integrated Pharmacophore-Guided Atom-Based 3D-QSAR, Molecular Docking, Virtual Screening, and ADMET Analysis for the Identification of Novel 1,3,4-Thiadiazole-Based Aldose Reductase Inhibitors

Priya Devi[1], Debarshi Mondal[2*], Shalini Sharma[3] and Harmel Singh Chahal[4]

[1]*Department of Pharmaceutical Chemistry, University School of Pharmaceutical Sciences, Rayat Bahra Professional University, Bohan, Nangal Shahidan, Hoshiarpur, PIN-146023, Punjab, India.*

[2]*Department of Pharmaceutical Chemistry, SWIFT School of Pharmacy, Ghaggar Sarai, Rajpura, Patiala, PIN-140401, Punjab, India.*

[3]*Department of Pharmaceutics, SWIFT School of Pharmacy, Ghaggar Sarai, Rajpura, Patiala, PIN-140401, Punjab, India.*

[4]*Department of Pharmacology, SWIFT School of Pharmacy, Ghaggar Sarai, Rajpura, Patiala, PIN-140401, Punjab, India.*

[*]debarshi9134@gmail.com (Corresponding Author)

RESEARCH ARTICLE **Open Access**

ARTICLE INFORMATION

Received: July 01, 2026
Accepted: July 27, 2026
Published Online: August 13, 2026

Keywords:
Aldose reductase inhibitors, 1,3,4-thiadiazole, Pharmacophore modelling, 3D-QSAR, Molecular docking

DOI: 10.15415/jptrm.2025.132007

ABSTRACT

Background: Chronic diabetic complications develop through the important role of aldose reductase (AR), a key enzyme in the polyol pathway. Clearly, it is important to identify potent AR inhibitors with better PK properties for treatment of diabetes-associated complications.

Purpose: The purpose of this study was to discover novel 1,3,4-thiadiazole derivatives as aldose reductase inhibitors using an integrated computational drug discovery approach.

Methods: The dataset consisted of 30 reported 1,3,4-thiadiazole derivatives, which were analysed by the pharmacophore modelling, atom-based three-dimensional quantitative structure-activity relationship (3D-QSAR), molecular docking, structure-activity relationship (SAR) analysis, R-group enumeration, virtual screening and ADMET prediction methods. Using the best pharmacophore model (AHHRR_1), a validated 3D-QSAR model was developed, and 1,419 new derivatives were designed. These compounds were then further optimised for binding interactions and pharmacokinetic parameters with the top-ranked ones, including the designed derivative PD01.

Results: The optimised pharmacophore and 3D-QSAR models were able to recognise the crucial structural elements that are essential for AR inhibition. Activity increased with the hydrophobic and electron-withdrawing groups, while the bulky polar groups were responsible for decreased activity. Docking studies showed that compounds 04 (-10.178 kcal/mol), 01 (-10.081 kcal/mol), 02 (-10.050 kcal/mol), 10 (-9.977 kcal/mol), and 11 (-9.672 kcal/mol) exhibited stronger binding than Epalrestat (-8.182 kcal/mol). The highest docking score was obtained for PD01 (-10.605 kcal/mol), which had strong hydrogen-bond, hydrophobic, π-π stacking, π-cation and halogen-bond interactions. The ADMET analysis showed good drug-likeness and good oral absorption.

Conclusion: The integrated computational workflow has concluded that PD01 is the most promising lead candidate with excellent binding affinity, a favourable interaction pattern and desirable ADMET properties. The results suggest that the scaffold 1,3,4-thiadiazole is a promising structural template for designing new generation aldose reductase inhibitors for diabetic complications.

1. Introduction

Diabetes mellitus (DM) is one of the most common chronic metabolic diseases in the world and defined by chronic hyperglycemia due to inadequate insulin production, insulin action, or a combination of the two. Diabetes mellitus is a significant health problem worldwide with an estimated prevalence of 589 million adult cases in 2024 and projected to increase to 853 million by 2050. The disease is estimated to cause a loss of life of 3.4 million individuals in 2024 and significant economic burden in terms of health care expenses and loss of productivity. Persistent hyperglycemia contributes to the development of microvascular and macrovascular complications, such as diabetic neuropathy, nephropathy,

retinopathy, cataracts, and cardiovascular diseases. While disease progression can be slowed by intensive blood sugar control, high blood sugar over time triggers multiple biochemical pathways that lead to tissue damage. The polyol pathway is one of the key pathways involved in the pathogenesis of diabetic complications, and aldose reductase (AR; AKR1B1; EC 1.1.1.21) is a therapeutic target that has been shown to be a good candidate for the development of new antidiabetic drugs (Brownlee, 2001; Oates, 2008; Srivastava *et al.,* 2005).

Aldose reductase is a cytosolic NADPH-dependent oxidoreductase of the aldo-keto reductase (AKR) superfamily. In physiological conditions, the enzyme is involved in the reduction of a large number of endogenous and exogenous aldehydes, playing a role in detoxification. But, in the hyperglycemic condition, a large amount of intracellular glucose is shunted from glycolysis into the polyol pathway, in which aldose reductase is the first and rate-limiting step, converting the glucose to sorbitol with the help of NADPH as a cofactor. Sorbitol is then converted to fructose through the activity of sorbitol dehydrogenase. Sorbitol poorly enters and exits cells, causing osmotic stress, and excess cellular uptake of sorbitol reduces the production of glutathione, which results in the formation of reactive oxygen species (ROS), inflammation, mitochondrial dysfunction, and advanced glycation end-product (AGE) formation. All of these pathological processes play an important role in the development of diabetic microvascular complications, such as diabetic retinopathy, diabetic nephropathy, diabetic neuropathy, and diabetic cataract (Figure 1) (Brownlee, 2001; Chung *et al*., 2003; Srivastava *et al.,* 2005).

Since aldose reductase is the first and the rate-limiting enzyme in the polyol pathway, pharmacological inhibition of this enzyme has proven to be effective in preventing or delaying diabetic complications without directly affecting insulin secretion or glucose uptake. Aldose reductase inhibitors (ARIs) inhibit the production of sorbitol, reduce the oxidative and osmotic stress, restore the intracellular antioxidant balance, and ultimately prevent tissue damage caused by hyperglycemia. Over the last few decades, a number of synthetic and natural ARIs have thus been studied. In the form of clinically developed inhibitors, epalrestat is the only drug that has been approved for clinical use in several Asian countries for the treatment of diabetic neuropathy, while sorbinil, tolrestat, zenarestat, zopolrestat, lidorestat, fidarestat, ranirestat, and ponalrestat were found to have good inhibitory activity, but these were not widely used because of their less favorable efficacy or pharmacokinetic properties or adverse effects like hepatotoxicity and hypersensitivity reactions (Figure 2). The restrictions still inspire the quest for safer and more effective aldose reductase inhibitors with better selectivity and pharmacological qualities (Oates & Mylari, 1999; Singh Grewal *et al.,* 2016; Balestri *et al.,* 2022).

The architecture of the active site of human aldose reductase has been extensively characterized by crystallographic and biochemical approaches and was well conserved in the enzyme. A catalytic pocket contains several important amino acid residues, including Tyr48, His110, Lys77, Asp43, Trp111, Trp20, Phe122, Trp219, Cys298, and Leu300, all of which contribute to the recognition of the substrate, proton transfer, hydrophobic stabilization, and NADPH-assisted reduction of carbonyl substrates. The effective inhibitors typically interact with the anion-binding pocket with several hydrogen-bonding and π–π stacking interactions and also bind to the specificity pocket *via* hydrophobic and van der Waals interactions with the conserved residues. Therefore, the introduction of the appropriate hydrogen-bond donor/acceptor groups along with aromatic and electron-withdrawing groups has been reported to improve binding affinity and the inhibitory activity against aldose reductase. The structural information has helped to rationalize the design of new inhibitors using contemporary computational-based drug discovery strategy (Shulgau *et al*., 2024).

The 1,3,4-thiadiazole nucleus has been shown to possess remarkable physicochemical and pharmacological properties with regard to its aldose reductase inhibitory activity and has received great importance among the various heterocyclic scaffolds that have been studied as aldose reductase inhibitors. The highly stable, lipophilic, and hydrogen-bonding abilities make the aromatic five-membered *N,S-heterocycle* an interesting privileged structure in medicinal chemistry. Several 1,3,4-thiadiazole derivatives have been shown to exhibit different biological activities such as antimicrobial, anticancer, anti-inflammatory, antioxidant, anticonvulsant, antiviral, and antidiabetic effects. Structural modification of the 1,3,4-thiadiazole framework, on the other hand, with various aromatic, heteroaromatic, and electron-withdrawing groups, has resulted in the discovery of potent aldose reductase inhibitors with improved enzyme selectivity and favorable binding interactions in the catalytic pocket. Structure-activity relationship (SAR) studies have also shown that the optimization of hydrophobic groups combined with hydrogen-bond donor and acceptor groups resulted in significant enhancement of inhibitory activity, and the scaffold is seen as a promising candidate for next-generation ARIs.

The discovery of enzyme inhibitors has been greatly advanced in recent years due to the use of computer-aided drug design (CADD), combining the two methods of ligand- and structure-based approaches. The pharmacophore modeling can be used to identify the crucial features needed for the biological activity, while three-

dimensional quantitative structure-activity relationship (3D-QSAR) analysis can be used to gain clues about the steric, electrostatic, hydrophobic, hydrogen-bond donor, and hydrogen-bond acceptor requirements for inhibitory potency. In addition to this, molecular docking provides a detailed understanding of the binding modes of the ligands to the protein and the essential intermolecular interactions in the protein active site, and virtual screening efficiently narrows down the search in large-scale chemical libraries to identify structurally different hit molecules. Furthermore, *in silico* ADMET prediction helps to assess PK and toxicity profile in early drug development, which helps to minimize the risk of drug failure in late stages of drug development. Their complementation has proved to be an effective method for discovering novel lead compounds with enhanced biological activity and drug-like properties, with an efficient and cost-effective strategy. Although there has been considerable research on aldose reductase inhibitors in the past years, numerous synthetic inhibitors that have been reported have not yet developed into drugs due to their poor efficacy, incompatibility with *in vivo* conditions, toxicity, or lack of enzyme specificity. In addition, there is no report on a systematic study of the SAR of 1,3,4-thiadiazole derivatives through integrated computational tools, and only a few reports have been published to combine pharmacophore modeling, 3D-QSAR, molecular docking, virtual screening, and prediction of ADMET into a single workflow. Hence, in the present study, pharmacophore modeling, atom-based and Gaussian field-based 3D-QSAR analyses, molecular docking, structure-activity relationship (SAR) analysis, virtual screening, molecular property prediction, and ADMET analysis were used to discover new 1,3,4-thiadiazole derivatives with the capacity to inhibit aldose reductase enzymes. This research work will give structural information that was expected to be useful in understanding the molecular basis of aldose reductase inhibitors and to help in the rational design of new aldose reductase inhibitors for the treatment of diabetes-associated complications (Ramunno *et al.*, 2012; Acar Çevik, *et al.*, 2023).

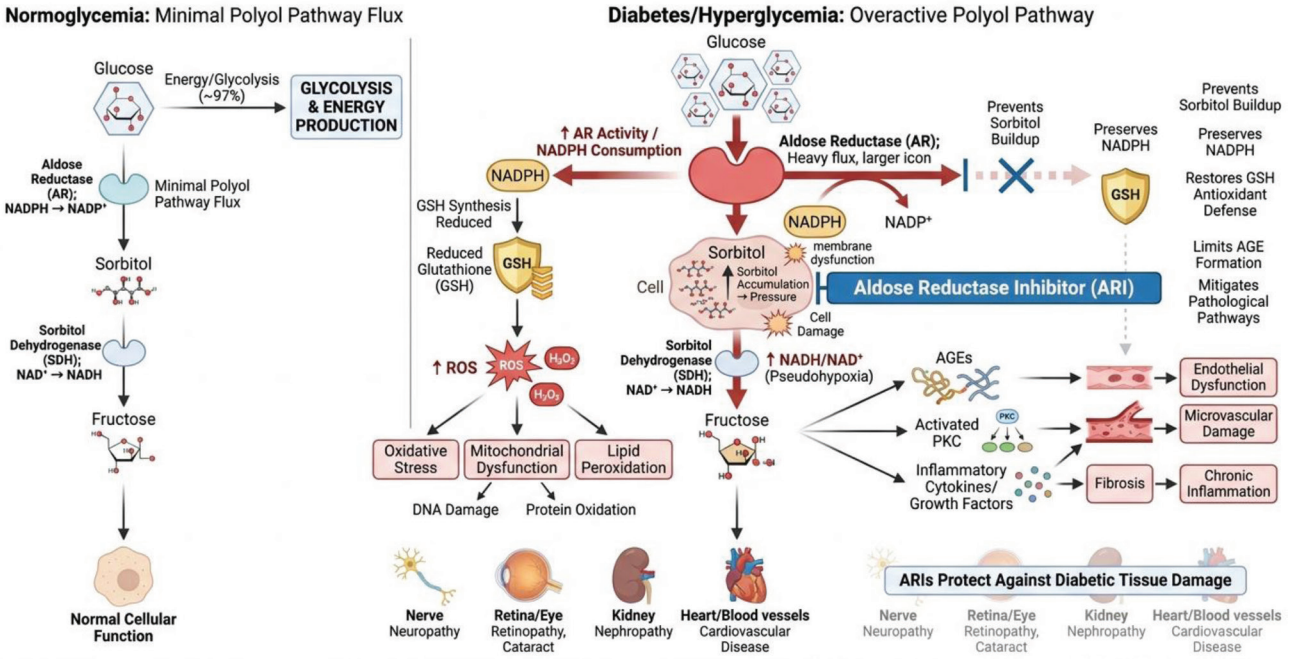

Figure 1: Mechanism of Action of Aldose Reductase

Various computational methods were applied for investigating a 30-compound data set that contains 1,3,4-thiadiazole analogues, and the obtained results were presented and compared with the literature-reported experimental results. Three-dimensional (3D) pharmacophore modelling was done to determine the crucial structural features for the inhibitory activity against aldose reductase. Later, the atom-based 3D quantitative structure-activity relationship (3D-QSAR) model was built to assess the roles that individual atomic features play in biological activity and to build a reliable predictive model. Molecular docking studies were performed to find out the active site of aldose reductase which was involved in stabilising the ligand during molecular interactions in the active site with favourable molecular interactions. In addition, a computational approach with integrated

pharmacophore modelling, atom-based 3D-QSAR analysis, molecular docking and virtual screening was used to identify and validate potential new inhibitors of aldose reductase. These complementary computational methods provided useful structural and biological information that can be used effectively to rationally design and optimise more potent aldose reductase inhibitors, as shown in Figure 3.

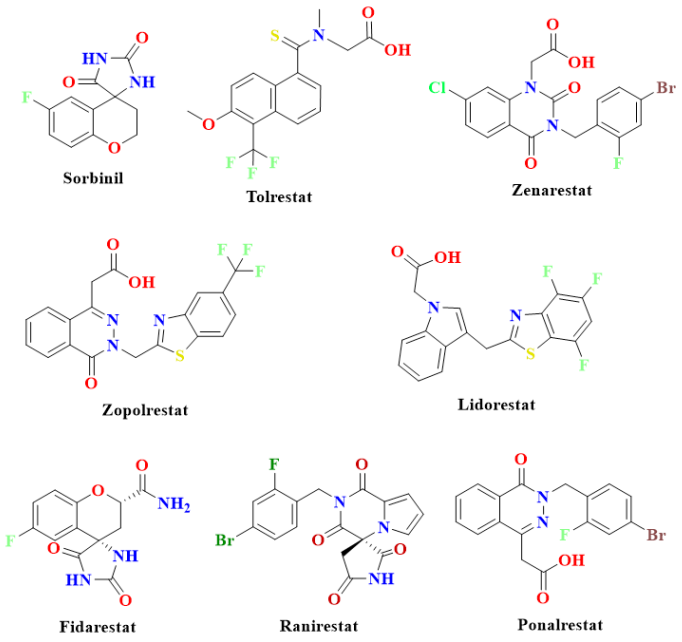

Figure 2: Schematic Representation of Drugs of the Aldose Reductase

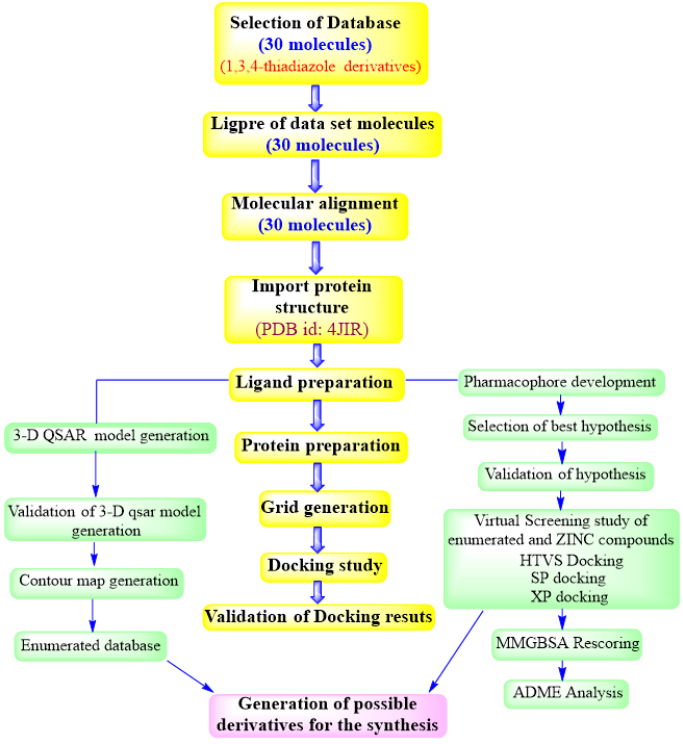

Figure 3: Workflow Describing the Computational Methods for the Discovery of Potential Aldose Reductase Inhibitors

2. Materials and methods

2.1. Selection of the Data Set and Preparation of Ligands

A set of 30 previously reported 1,3,4-thiadiazole derivatives that have aldose reductase inhibitory activity were chosen for computational study. The chemical structures were first drawn in two dimensions (2D) and taken from published literature, then redrawn with ChemDraw Professional 16.0 (Cambridge, MA, USA). These structures were then modified to 3D structures and energy minimized to achieve stable structures for further computational studies. The experimentally reported IC_{50} values were converted to the corresponding pIC_{50} values (6.721-7.696) for 3D quantitative structure-activity relationship (QSAR) modeling. All compounds shared a common 1,3,4-thiadiazole backbone, and the changes in the substituents are shown in Table 1, along with their IC_{50} and pIC_{50} values. For developing and externally testing the 3D-QSAR models, the entire data set was randomly split into an 80% training set and a 20% test set. Five partial least squares (PLS) components were used to build up the predictive models using the selected pharmacophore hypothesis. All the molecules were subjected to energy minimization and placed on a common molecular framework to ensure that all molecules are oriented in the same manner in space before modeling, thus increasing the accuracy and reliability of the QSAR analysis (Figure 4) (Akdağ *et al.,* 2025; Kaya *et al.,* 2025; Kaya *et al.,* 2024).

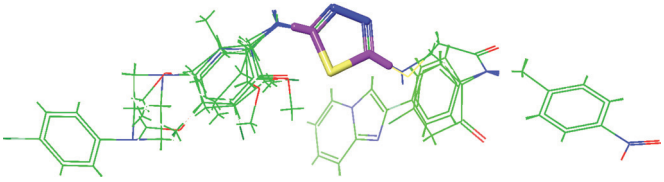

Figure 4: Alignment of dataset molecules

2.2. Alignment of the Dataset

Structural alignment is an important factor of building a reliable 3D-QSAR model because it guarantees the generation of the molecular field descriptors accurately. If the molecules are aligned correctly, all the molecules will be in the same 3-D orientation, and it will allow for meaningful comparison of structural features and for better correlation of molecular structure to biological activity. However, if there is poor alignment, the predictive ability and reliability of the QSAR can also be diminished. A flexible ligand alignment approach was used in the present study to generate an optimal common alignment of all dataset compounds using the Automatic Reference Alignment option available in Schrödinger Maestro version 12.5. The alignment of the molecules was done according to the chosen pharmacophore hypothesis; the selected model was able to be used to build the atom-based 3D-QSAR model. The final aligned conformations for all the compounds developed for the model are shown in Table 1 and in Figure 4 (Bisht *et al.*, 2025).

Table 1: Description of Substitutions on the Core Moiety with IC_{50} and pIC_{50} Values

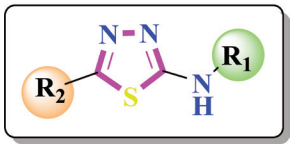

Comp.	R1	R2	IC50 (nM/µm)	pIC50 (µm)
01	CH_3	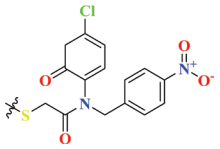	37.02 nM	7.432
02		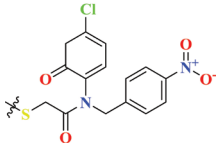	82.73 nM	7.082

03		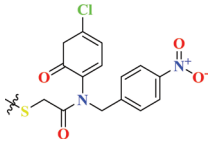	103.1 nM	6.987
04		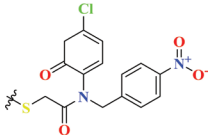	175.4 nM	6.756
05		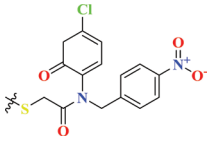	61.41 nM	7.212
06		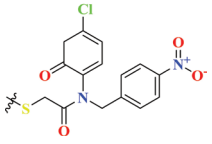	26.53 nM	7.576
07		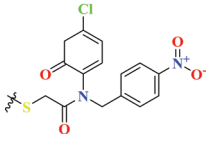	49.76 nM	7.303
08		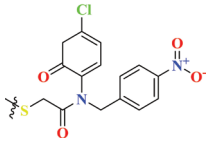	87.72 nM	7.057
09		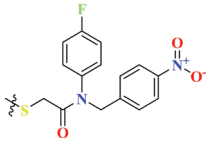	53.76 nM	7.270
10		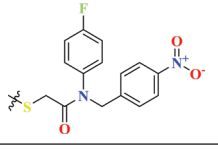	68.29 nM	7.166
11		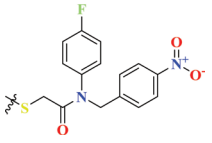	125 nM	6.903
12		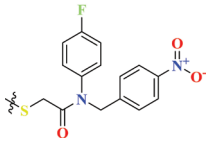	61.03 nM	7.214

13		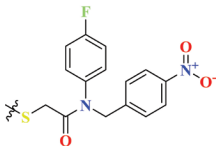	64.37 nM	7.191
14		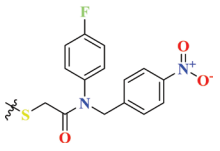	55.05 nM	7.259
15		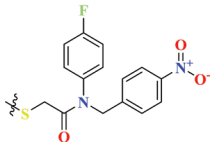	20.16 nM	7.696
16		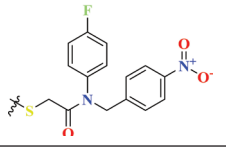	34.99 nM	7.456
17		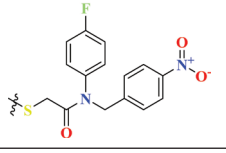	59.38 nM	7.226
18		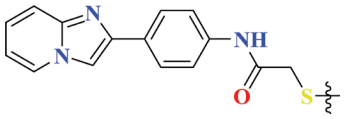	34.91 nM	7.457
19		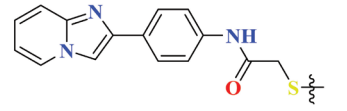	74.16 nM	7.130
20		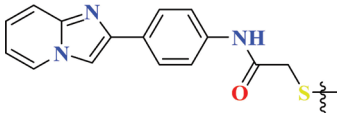	139.6 nM	6.855
21		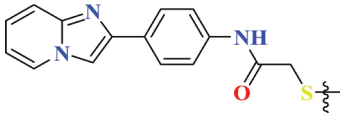	78.53 nM	7.105
22		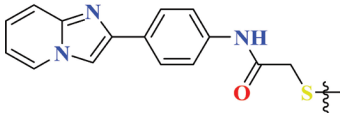	44.29 nM	7.354
23		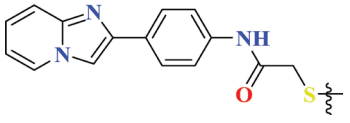	23.47 nM	7.629

24		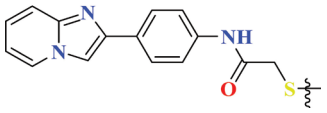	71.35 nM	7.147
25		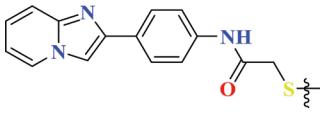	45.35 nM	7.343
26	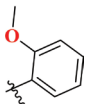	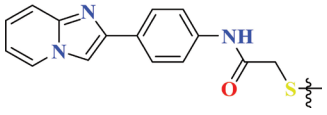	80.32 nM	7.095
27		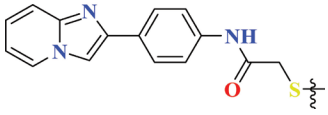	69.87 nM	7.156
28		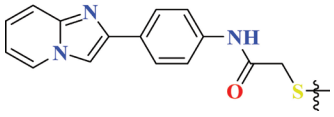	97.78 nM	7.010
29	CH_3	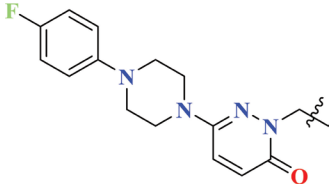	0.094	7.027
30	CH_3	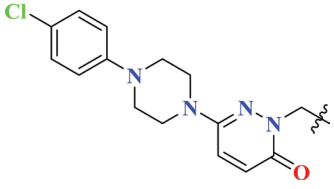	0.19	6.721

2.3. Transformation of IC50 and Selection of Test and Training Set

The biological activities of the selected 1,3,4-thiadiazole derivatives were reported as IC_{50} values in nM or µM. All IC_{50} values were converted to pIC_{50} values using the Calculator module of Schrödinger Maestro version 12.5 ($pIC_{50} = -\log_{10}(IC_{50})$) to standardize the data for quantitative analysis and for better accuracy of the 3D-QSAR study. The pIC_{50} values were then calculated and used as the dependent variable in developing the 3D-QSAR models. The IC_{50} values calculated in the model were offset by 6 or 9 to prevent negative activity values from being produced when the model was created, depending on the unit of the original IC_{50} value. The aligned molecular dataset was then randomly split into training and test sets so that 80% of the molecules were used for the construction of the QSAR models, and the remaining 20% of molecules were used for the assessment of the predictive performance and external validation of the models as shown in Table 1 (Bisht *et al.,* 2025; Verma *et al.,* 2021).

2.4. Generation of 3D-QSAR Model

The aligned molecular dataset (Table 2) was used to independently develop the atom-based 3D-QSAR models using Schrödinger Maestro version 12.5. The grid was used with the spacing of 1.0 Å, and during the model generation, the molecular grid was expanded 3.0 Å beyond the limits of the training set to cover the entire molecular features. To avoid making unrealistic contributions to energy parameters, force-field interactions up to 2.0 Å from any atom in the training molecules were not included, and steric and electrostatic energy values were capped at 30.0

kcal/mol. Variables with a standard deviation less than 0.01 were deemed to be unimportant and excluded from analysis to enhance the robustness of the model. The leave-one-out (LOO) cross-validation approach was used to assess the predictive performance of the model. Four partial least squares (PLS) factors were used to build the atom-based 3D-QSAR model. Significant molecular descriptors such as hydrogen bond donor (HBD), hydrophobic (nonpolar), and electron-withdrawing (EWG) groups were used to explain and predict the aldose reductase inhibitory activity of 1,3,4-thiadiazole derivatives (Bisht *et al.,* 2025; Verma *et al.,* 2021; Veerasamy *et al.*, 2011).

Table 2: Generation of 3D-QSAR Model - Actual pIC_{50}, Predicted $pIC_{50,}$ and Residual Values

Comp. No.	**Actual pIC**50 **(x)**	**Atom Based**	
		Predicted pIC50	**Residuals**
		(Ÿ)	(Ÿ -X)
1	7.432	7.242	-0.190
2	7.082	7.167	0.001
3	6.987	6.978	0.075
4	6.756	7.336	0.122
5	7.212	7.055	-0.136
6	7.576	7.262	0.003
7	7.303	7.604	-0.092
8	7.057	7.473	0.017
9	7.270	7.277	0.051
10	7.166	7.391	-0.066
11	6.903	6.950	-0.180
12	7.214	6.969	-0.113
13	7.191	6.950	0.095
14	7.259	7.319	0.214
15	7.696	7.319	-0.035
16	7.456	7.391	-0.238
17	7.226	7.346	0.199
18	7.457	7.359	0.016
19	7.130	7.346	0.251
20	6.855	7.259	0.103
21	7.105	7.018	0.008
22	7.354	7.195	0.208
23	7.629	6.910	0.154
24	7.147	7.113	-0.099
25	7.343	7.532	-0.044
26	7.095	7.336	0.033
27	7.156	7.113	0.056
28	7.010	7.353	0.083
29	7.027	6.918	-0.109
30	6.721	6.839	0.118

(*) is a denoted atom-based test set

2.4.1. Partial Least Squares (PLS)/3D-QSAR Model Evaluation of Atom-Based

Partial least squares (PLS) regression analysis was used to determine the relationship between the experimental pIC_{50} values (dependent variables) and the atom-based 3D-QSAR molecular field descriptors (independent variables). The quality, predictive ability, and statistical reliability of the developed QSAR models were assessed using various validation parameters such as coefficient of determination (R^2), cross-validated coefficient (Q^2), leave-one-out (LOO) cross-validation, R^2 scramble, cross-validated R^2 (R^2CV), F-test, root mean square error (RMSE), p-value, Pearson correlation coefficient (Pearson-r), and standard deviation (SD), as summarized in Table 3. The following parameters were considered to be prerequisites of a statistically robust and reliable QSAR model: good internal consistency and predictive ability (difference between R^2 and Q^2 < 0.3), good external consistency and predictive ability (SD < 0.5), RMSE near zero, and R^2 between 0.6 and 1.0. Moreover, the high F-value and low p-value indicated the statistical significance of the regression model, and the high Pearson correlation coefficient indicated that the developed atom-based 3D-QSAR model had excellent agreement between the predicted and experimental activities, demonstrating the robustness and predictive power of the developed atom-based 3D-QSAR model (Bisht *et al.,* 2025; Gholami Rostami & Fatemi, 2018; Gholami Rostami & Fatemi, 2019; Singh *et al.,* 2022).

Table 3: Pharmacophore Hypothesis Development with Scores and their Ranking

PLS Statistics	Reference Values	Atom Based
SD	SD of regression < SD of actual activities	0.123
R^2	> 0.6	0.743
R^2_{CV}	> 0.5	0.798
$R^2_{Scramble}$	> 0.5	0.863

F	Larger values of F	143.7
P	The lesser the values of P, the greater the degree of confidence	8.01e-05
RMSE	Close to 0	0.16
Q^2	> 0.5, and (R^2 - Q^2) < 0.3	0.714
Pearson-r	Close to 1, lesser scattered predictive activities in the plot of observed *Vs.* predicted activities	0.884

2.4.2. Contour Map Generation

To explore the effect of various molecular properties around the 1,3,4-thiadiazole scaffold on the predicted aldose reductase inhibitory activity, atom-based 3D-QSAR contour maps were used. The contour analysis was used to investigate the spatial distribution of important molecular properties such as hydrogen bond donor (HBD), hydrophobic (nonpolar), and electron-withdrawing (EWG). The coloured contour regions represent the locations of biological activity that would be favoured or unfavoured by certain structural changes. In the positive contour regions, suitable functional groups are to be introduced to increase the binding affinity and aldose reductase inhibitory activity with the favourable regions. Negative contour regions, on the other hand, suggest less favourable positions, in which similar substituents added to the protein will diminish the protein-ligand interactions and in turn lessen biological activity. Thus, the contour maps are useful to understand the preferred and unfavourable substitution pattern around the 1,3,4-thiadiazole nucleus and can be used as a guide for the rational design and optimisation of more potent aldose reductase inhibitors (Stitou *et al.,* 2021; Vishwakarma *et al.,* 2021; Ahmed *et al.,* 2024).

2.4.3 External Validation of 3D-QSAR Model

The developed 3D-QSAR model was also externally validated using an independent and structurally diverse test set to assess its predictive ability. The finalised model was applied to predict the biological activity of the test compounds, and the predicted pIC_{50} values were correlated with the experimental ones to check the robustness and prediction accuracy of the model. Several statistical parameters were used for external validation, such as the predictive correlation coefficient (r^2pred), the slopes of the regression lines (k and k′), the coefficients of determination through the origin (R_0^2 and $R'_0{}^2$), and the modified squared correlation coefficients [r^2m (LOO), r^2m, and r'^2m]. These validation parameters were used as criteria to establish good external predictive ability in a QSAR model. A predictive correlation coefficient (r^2pred) > 0.6 was obtained, which showed that the developed model was statistically sound and reliable and had a good predictive capability for the aldose reductase inhibitory activity of structurally diverse 1,3,4-thiadiazole derivatives (Asati *et al.*, 2017).

a) $$\left(r^2 - R_0^2\right)/r^2 < 0.1, \left(r^2 - R_0'^2\right)/r^2 < 0.1.$$

b) $$0.85 < K < 1.15 \, or \, 0.85 < K' < 1.15.$$

c) $$r^2 m > 0.5.$$

2.5. Pharmacophore Development

To find the essential molecular features of the selected 1,3,4-thiadiazole derivatives for their aldose reductase inhibitory activity, pharmacophore modelling was carried out. The structural features of the compounds were correlated with the experimentally reported pIC_{50} values to develop the pharmacophore hypotheses. The PHASE module implemented in Schrödinger Maestro version 12.5 was used for pharmacophore generation. The compounds were divided into three groups based on their biological activities, the active (10-15%), inactive (25-30%), and intermediate groups. All the pharmacophores were generated with a box size of 1 Å and inter-site minimum distance of 2 Å, with the default values of the software. Hydrogen bond acceptors (A), hydrogen bond donors (D), hydrophobic groups (H), aromatic rings (R) and positively/negatively ionisable groups (p□) or (p□). A total of 20 pharmacophore hypotheses were generated in which AHHRR_1 was found to be the best. This model featured two hydrogen bond acceptors (A), one hydrophobic group (H), one hydrogen bond donor (D) and one aromatic ring (R) (Figure 5). Various representative compounds for each active compound (4, 1, 2, 10 and 11), inactive compounds (13 and 15) and intermediate compounds (18, 29, 22, 27 and 20) were utilised in the pharmacophore model development. The obtained hypotheses were then statistically and geometrically analysed with various parameters such as survival score, site score, vector alignment, volume overlap, inactive match, and receiver operating characteristic (ROC) analysis to select the most reliable and predictive pharmacophore model for further 3D-QSAR modelling and virtual screening (Figure 5) (Bisht *et al.,* 2025; Vanajothi *et al.,* 2020).

2.6. R-group Enumeration for New Compound Generation

To systematically prepare structurally diverse 1,3,4-thiadiazole derivatives, the R-group enumeration

method was used to systematically replace the groups attached to the parent structure with chemically meaningful groups. The atom-based 3D-QSAR model was used as a guide for the design of these new analogues, highlighting desirable substitution sites and the molecular characteristics that are necessary for enhancing aldose reductase inhibitory activity. The core scaffold of 1,3,4-thiadiazole was kept throughout the design process in order to maintain the core structure of the molecule. The analysis of the contour map, then, led to the inclusion of a range of R1 substituents at appropriate locations in the binding pocket to enhance interactions with the enzyme and appropriate R2 substituents to improve relevant physicochemical properties such as solubility, binding affinity, and overall molecule stability (Figure 6). The substituents chosen were carefully selected to give the appropriate balance of hydrogen bond donor and hydrogen bond acceptor functions, which would allow good interactions with key amino acid residues in the enzyme active site. Based on this rational design approach, a virtual library consisting of 1419 R-group-enumerated derivatives was generated and then screened for novel compounds with better aldose reductase inhibitory activity using the Schrödinger Suite (Schrödinger LLC, New York, NY, USA) (Figure 6) (Gupta *et al.,* 2025; Sharma *et al.,* 2025; Polya *et al.,* 2012).

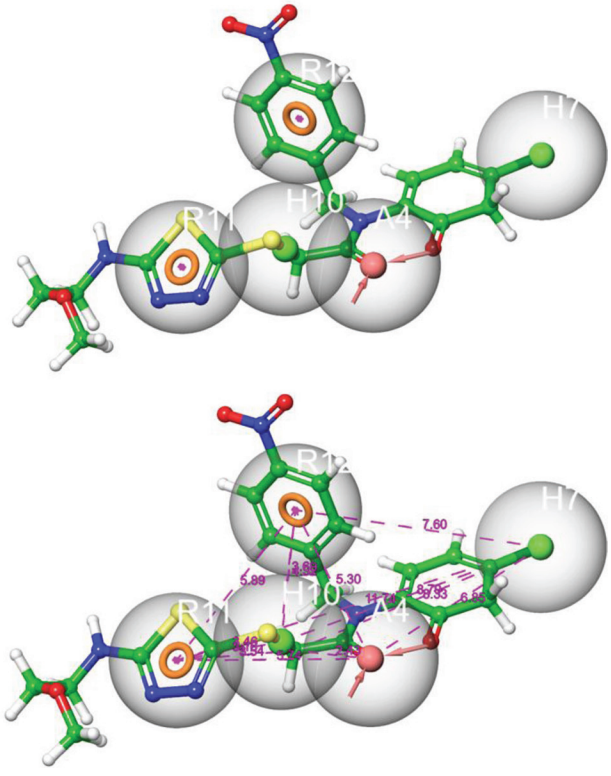

Figure 5: Best Pharmacophoric Hypothesis AHHRR_1

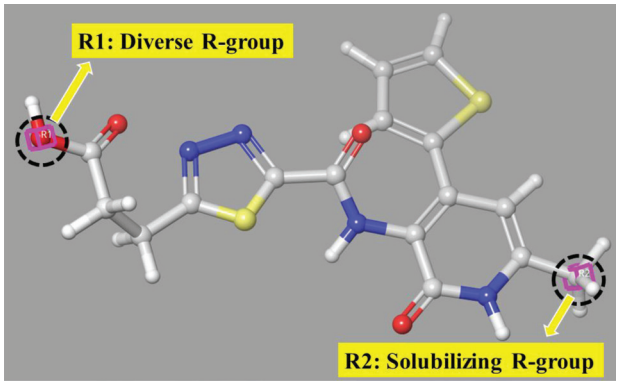

Figure 6: Substitution of R-position Enumeration for New Compounds Generation

2.7. Virtual Screening of R-group-Enumerated Compound Generation

A virtual library of 1,419 R-group-enumerated 1,3,4-thiadiazole derivatives was created and screened using virtual screening to find new lead molecules with better inhibitory activity on aldose reductase. The 3D structure of all designed molecules was generated after importing into Schrödinger Maestro version 12.5 and energy minimized using the OPLS4 force field to obtain stable molecular conformation before screening. The optimized compound library was then tested by a hierarchical molecular docking strategy with the Glide module. The docking protocol was validated prior to virtual screening with the most active reported 1,3,4-thiadiazole derivative as a reference ligand. All the listed compounds were docked in the aldose reductase active site with High Throughput Virtual Screening (HTVS) mode with flexible ligand sampling for fast identification of the possible binders. The top-ranked compounds of the HTVS stage were re-docked using the Standard Precision (SP) protocol in order to enhance the docking accuracy. Finally, the top-performing compounds from the SP stage were docked again using Extra Precision (XP) docking to generate more accurate docking poses, interaction profiles, and docking scores. The compounds that gave the better XP docking score were then tested in the validated three-dimensional atom-based model for drug design. The 3D-QSAR model was used to predict the biological activity of the compounds and for selecting the most promising lead molecules for further structural optimization and development as aldose reductase inhibitors (Sharma *et al.*, 2025).

2.8. Molecular Docking

The binding mode and molecular interactions of the selected 1,3,4-thiadiazole derivatives with aldose reductase (AR) were

investigated through molecular docking studies and evaluated using the Glide module in Schrödinger Maestro version 12.5. The 3D structure of aldose reductase (PDB ID: 4JIR, Resolution: 2.00 Å) was retrieved from the RCSB Protein Data Bank. Protein structure was prepared using the Protein Preparation Wizard, which includes missing hydrogen atoms, assigning correct bond orders, removing crystallographic water molecules not involved in the binding of the ligands, and energy minimization using the OPLS4 force field. The receptor grid was created with a resolution of 20 Å centered on the co-crystallized ligand, X = -6.03, Y = 8.85, and Z = 17.22, which represents the active binding site for docking. The LigPrep module was used to prepare the low-energy, geometry-optimized three-dimensional conformations of the ligand structures before docking. All the prepared ligands were then docked into the aldose reductase binding site using the Extra Precision (XP) docking protocol with flexible sampling of the ligand to get accurate ligand poses and docking scores. Moreover, blind docking was carried out to look for any alternative binding sites on the protein surface. Finally, the resulting protein–ligand complexes were analyzed using XP Visualizer to see the key interactions with the ligand, such as hydrogen bonding, π–π stacking, π–cation, halogen bonding, and hydrophobic interactions that are essential for the recognition and stabilization of the ligand in the active site of Aldose Reductase (Yadav *et al.,* 2021; Cevik *et al.,* 2023) (Figure 7).

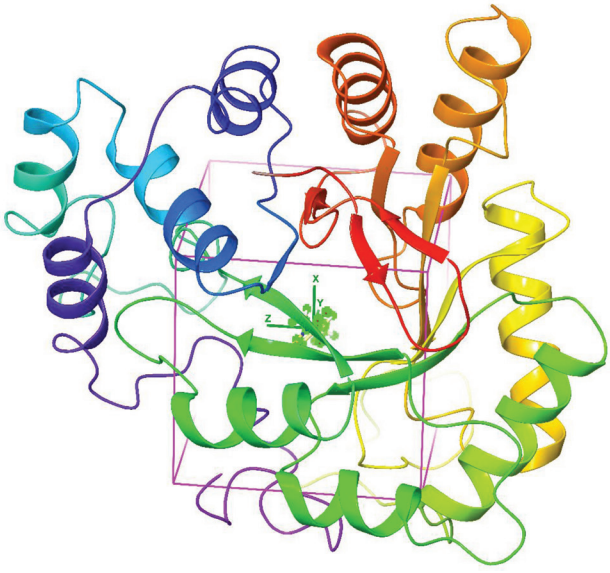

Figure 7: Generated Grid within the Aldose Reductase

2.9. ADME Prediction

Using the QikProp module built into Schrödinger Maestro version 12.5, the Absorption, Distribution, Metabolism, and Excretion (ADME) parameters of the chosen 1,3,4-thiadiazole derivatives were predicted. Drug-like properties of the compounds were assessed by the following significant pharmacokinetic descriptors: molecular weight (MW), hydrogen bond donors (HBD), hydrogen bond acceptors (HBA), dipole moment, rotatable bonds, and predicted human oral absorption (HOA). Predicted aqueous solubility (QPlogS) and predicted skin permeability (QPlogKp) were also calculated and used to estimate the pharmacokinetic behavior of the compounds. The overall drug-likeness of each molecule was also calculated based on Lipinski's Rule of Five, which assesses important molecular properties such as the number of hydrogen bond donors and acceptors, lipophilicity, molecular weight, etc. related to good oral bioavailability. These predictions offer useful insights in the selection of compounds that potentially have good pharmacokinetic properties and drug-like characteristics for development as aldose reductase inhibitors (Hosen *et al.,* 2017; Inamdar *et al.,* 2023; Haritha *et al.,* 2024; Acar Çevik et *al., 2023).*

3. Results and Discussion

3.1. Data Set of Top Pharmacophore Hypotheses

A total of 20 pharmacophore hypotheses were developed to determine the key molecular features, which are crucial for aldose reductase inhibitory activity. The following statistical and geometric scoring parameters were used to assess these hypotheses, and the results are summarized in Table 4. From all the generated models, the model Hit 1, which is the AHHRR_1 pharmacophore hypothesis, was chosen as the reliable one since it exhibited the best correlation between the chosen pharmacophoric features and the experimental biological activities. The AHHRR_1 model performed best with respect to both survival and the hypothesis score, suggesting that it was the best model for predicting survival and for further computational studies. The pharmacophore model consists of two hydrogen bond acceptors (A), one hydrophobic feature (H), one hydrogen bond donor (D), and one aromatic ring (R), which collectively represent the structural requirements for the effective inhibition of aldose reductase. In addition, the Schrödinger Maestro software's Distance Computation tool was used to calculate inter-feature distance and spatial arrangement of the selected AHHRR_1 model. The distance map (Table 5) obtained in this way was a geometric description of the relationship between the pharmacophoric features and can be used to provide a safe structure-based guidance framework for the molecular alignment and further development of the atom-based 3D-QSAR model.

Table 4: Pharmacophore Hypothesis Development with Scores and their Ranking

HypoID	Survival	Site	Vector	Volume	Select	Matches	Inactive	Adjusted	BEDROC	RefLig
AHHRR_1	5.0384	0.7587	0.928	0.7578	1.8949	5	1.6172	3.4212	1	mol_3
AHHRR_2	4.8347	0.7646	0.7891	0.6824	1.8997	5	1.4985	3.3362	0.954	mol_1
ADHRR_1	4.7832	0.6175	0.9353	0.6145	1.9169	5	1.505	3.2781	0.9962	mol_2
ADHHR_1	4.7821	0.7037	0.9432	0.4828	1.9534	5	1.8331	2.949	0.9849	mol_3
AHHRR_3	4.6979	0.6367	0.8051	0.657	1.9001	5	1.7751	2.9228	1	mol_1
ADHRR_2	4.689	0.6112	0.8649	0.5904	1.9236	5	1.433	3.2561	0.9702	mol_1
ADHRR_3	4.6628	0.5824	0.8717	0.6129	1.8969	5	1.4648	3.198	0.9924	mol_1
DHHRR_1	4.6558	0.47	0.8029	0.5782	2.1058	5	1.5397	3.1161	1	mol_3
ADHHR_2	4.6542	0.6787	0.9363	0.4048	1.9355	5	1.6852	2.9691	1	mol_4
AHHRR_4	4.623	0.5728	0.8641	0.6017	1.8855	5	1.6965	2.9265	0.9924	mol_5
AHHR_1	4.5846	0.8904	0.9516	0.6906	1.3531	5	1.598	2.9866	0.9886	mol_1
DHHR_1	4.4673	0.8688	0.9817	0.4031	1.5148	5	1.7696	2.6978	0.9886	mol_4
AHHR_2	4.408	0.8711	0.9027	0.6042	1.331	5	1.8986	2.5094	1	mol_5
AHHR_3	4.4051	0.7959	0.9542	0.6116	1.3445	5	1.8077	2.5974	1	mol_5
HHRR_1	4.405	0.6375	0.8922	0.6688	1.5076	5	1.5884	2.8166	0.9745	mol_1
AHRR_1	4.3907	0.7846	0.8676	0.6764	1.3631	5	1.6617	2.729	0.8779	mol_1
DHHR_2	4.3808	0.7969	0.9646	0.4126	1.5077	5	1.7829	2.5979	0.975	mol_4
AHHR_4	4.337	0.8642	0.8913	0.5354	1.3472	5	1.8068	2.5302	0.9962	mol_1
ADHR_1	4.3349	0.8319	0.9397	0.5137	1.3506	5	2.0773	2.2576	1	mol_1
AHRR_2	4.3179	0.7671	0.8771	0.593	1.3818	5	1.6596	2.6583	0.8418	mol_1

Table 5: Distance Mapping of Best Pharmacophoric Hypothesis AHHRR_1

AADHR_3	Features Type	X	Y	Z
A4	H- bend acceptor	-0.26	2.25	-0.87
H7	Hydrophobic	-4.00	6.83	2.59
H10	Hydrophobic	-0.89	0.00	0.00
R11	Aromatic ring	1.89	-2.99	0.01
R12	Aromatic ring	-0.45	0.89	4.20

3.2. Validation of Pharmacophore Model

To further assess the predictive ability of the selected pharmacophore hypothesis, receiver operating characteristic (ROC) and percentage screen analysis were carried out. The percentage screen analysis gives an idea about how well the pharmacophore model can predict the activity of the compounds from the whole set, while the ROC curve represents the relationship between the sensitivity and the specificity of the classification of the pharmacophore model at different threshold values. The objective of an ideal pharmacophore model was to fully separate active molecules from inactive molecules and get the ROC curve to the upper left side of the graph with 100% sensitivity and 100% specificity. The pharmacophore hypothesis selected (AHHRR_1) showed a very good classification performance with area under the ROC curve (AUC) and ROC value (Figure 8). The values obtained showed that the model's discriminatory power was high and it could accurately classify the compounds as active and inactive, indicating the robustness of the model and its suitability for further 3D-QSAR modelling and virtual screening studies.

3.3. Analysis of 3D-QSAR Validation

This atom-based 3D-QSAR analysis created a valuable dataset that was applied to formulate and validate predictive models for aldose reductase inhibitory activity. The biological activities (pIC_{50}) of all the compounds are given in terms of experimental and predicted values

in Table 6. The performance and statistical reliability of the models developed were evaluated by various statistical parameters such as the coefficient of determination (R^2), the cross-validated coefficient (Q^2), the standard deviation (SD), the F-test, the p-value, the root mean square error (RMSE), and the Pearson correlation coefficient (Pearson-r). The high R^2 value, Q^2 value, F-test, and high Pearson r value, along with low SD, RMSE, and p-values, suggest high model accuracy and predictive power of a robust and predictive QSAR model. Table 7 presents the statistical results obtained with four partial least squares (PLS) factors. The first models had comparatively lower R^2, Q^2, and R^2 scramble values, meaning that they did not have a good predictive power. A model with improved statistical quality was obtained by optimization of the atom-based model for 3D-QSAR, and it was selected as the final predictive model. Important molecular descriptors such as hydrogen bond donor (HBD), hydrophobic (nonpolar), and electron-withdrawing (EWG) groups were incorporated into this model, and their individual contributions to the biological activity were represented by visualizing the atom-type fraction map. The scatter plot of the experimental and theoretical values of pIC_{50} for the training set compounds (Figure 9) revealed that most of the data points were tightly grouped around the regression line passing through the origin, indicating good agreement between the experimental and predicted pIC_{50} activities. The developed 3D-QSAR model has been found to be robust, statistically reliable, and highly predictive in designing new 1,3,4-thiadiazole-based aldose reductase inhibitors, and these results further validate the developed model.

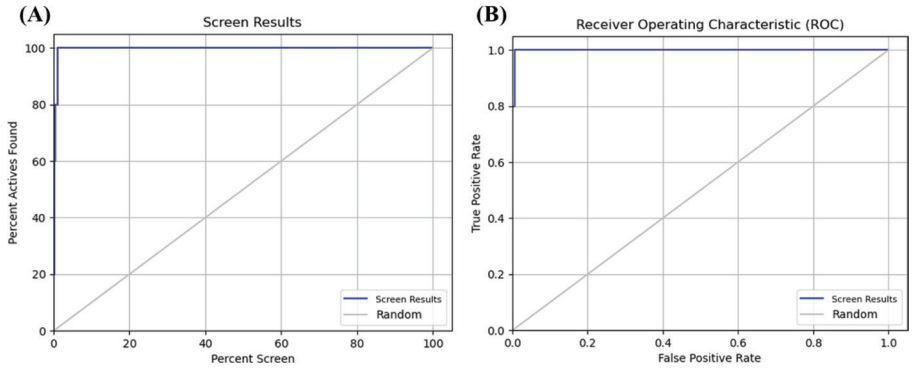

Figure 8: Validation of Pharmacophore Model (A) Percent plot; (B) ROC plot

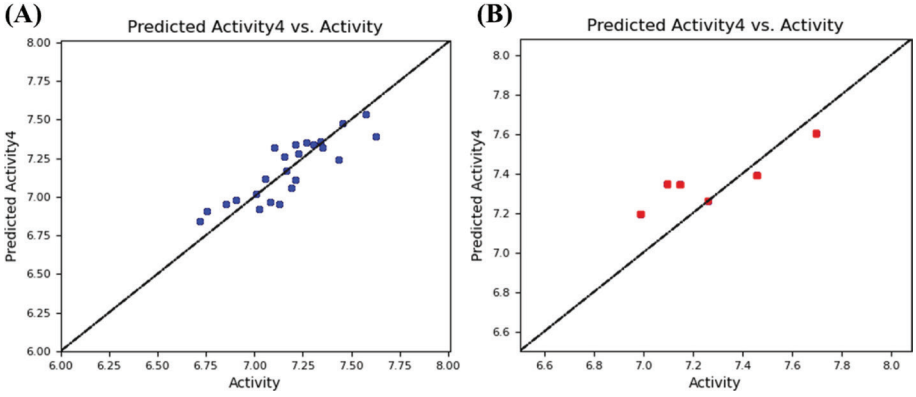

Figure 9: Graph Shows the Relationship Between the (A) Training and (B) Test Set Data's Actual and Predicted IC_{50} Values (Atom Based)

3.4. Evaluation of Contour Map

3.4.1. Atom-based 3D-QSAR Models

The influence of hydrogen bond donor (HBD), electron-withdrawing group (EWG), and hydrophobic (non-polar) molecular features on the inhibitory activity of the selected 1,3,4-thiadiazole derivatives for aldose reductase was investigated using an atom-based 3D-QSAR model. It offers a clear understanding of the role of each atomic component in the biological activity, and it can be used as a reliable predictor of the activity of structurally related compounds. The statistics of the atom-based 3D-QSAR model developed are given in Table 7. In order to understand the structure-activity relationship, contour maps were created to delineate favorable

and unfavorable spatial regions that affect aldose reductase inhibition. The contour maps of the 3D-QSAR analysis showed that the hydrophobic (nonpolar) field contributed the most to the inhibitory activity of aldose reductase, followed by the electron-withdrawing (EWG) field and finally, the hydrogen bond donor (HBD) field (Figure 10). The results showed that the hydrophobic interactions are the major factor contributing to the increased binding affinity and inhibitory potency of 1,3,4-thiadiazole derivatives, and the suitable electron-withdrawing groups accentuate further biological activity. Hydrogen bond donor groups, on the other hand, although they interact with the active site residues, don't make a significant contribution to the inhibition of aldose reductase in comparison to hydrophobic and electron-withdrawing groups. Therefore, such conformational modifications to optimize favorable hydrophobic interactions with the enzyme, combined with the judicious placement of electron-withdrawing groups at strategic positions, are potential strategies to design more potent aldose reductase inhibitors.

3.4.1.1. Hydrogen Bond Donor Features

The remaining 3D-QSAR contour map for the Hydrogen Bond Donor (HBD) group shows the space occupied by the hydrogen-bond donor groups, which affects the inhibition activity of Aldose Reductase (AR) by 1,3,4-thiadiazole derivatives. The blue cubes on the contour map represent favorable (positive) positions: hydrogen bond donor groups at these positions are likely to increase the binding affinity of the molecule by making strong hydrogen bond interactions with key amino acid residues that exist at the active site of aldose reductase. These substitutions are thus expected to enhance enzyme inhibition and biological activity. The yellow contour cubes, on the other hand, denote the less favorable (negative) regions in which the presence of hydrogen-bond donor (HBD) groups is expected to lower the inhibitory activity. In the current atom-based 3D-QSAR model, these yellow contour cubes are mainly distributed around the various regions, including the terminal heterocyclic ring, the substituted amino linker, and the opposite terminal part of the molecule. The distribution shows that the addition of hydrogen-bond donor groups in these regions may not be beneficial for the inhibitory activity of Aldose Reductase (AR) and should be avoided in the rational design of more potent 1,3,4-thiadiazole derivatives. These areas may contain hydrogen bond donor groups that limit the inhibitory activity due to steric hindrance or improper orientation or unfavorable interaction within the binding site. Thus, substituents with hydrogen bond donating ability should be avoided and/or minimized in these yellow areas, while the effect of introducing suitable hydrogen bond donors in the blue favorable areas could be beneficial in designing more potent inhibitors of aldose reductase (Figure 10A).

3.4.1.2. Hydrophobic/Non-Polar Features

The 1,3,4-thiadiazole derivatives were designed, and the hydrophobic (nonpolar) contour map derived from the atom-based 3D-QSAR model explains the spatial areas where the hydrophobic substituents have a significant contribution to the aldose reductase (AR) inhibitory activity of the designed 1,3,4-thiadiazole derivatives. The contour map shown above was for guidance only, and light green cubes indicate favorable (positive) regions: it was expected that the incorporation of hydrophobic substituents (e.g., methyl, ethyl, propyl, isopropyl, tert-butyl, cycloalkyl, or aromatic groups) at these positions will improve inhibitory activity. It was noticed that there was a huge group of contours in light green color around the left-side alkyl chain attached to the amino linker, which strongly favors hydrophobic interactions. Besides that, light green contour cubes were seen around the central linker and near the fused heterocyclic ring, which showed the efficient regions of the molecule for the insertion of moderately hydrophobic groups that were expected to increase the binding affinity of the ligand and inhibit the activity of aldose reductase (AR). The hydrophobic groups can make better interactions with the nonpolar part of the aldose reductase active site through favorable hydrophobic and van der Waals interactions, which will lead to enhanced binding affinity and inhibitory potency. Red cubes are unfavorable (negative) regions, where bulky hydrophobic substituents may be expected to decrease biological activity. The atom-based 3D-QSAR model showed that hydrophobic groups with a bulky nature at the end of the alkyl chain, near the central linker and the heterocyclic ring, are unfavorable, which means that they can cause steric hindrance, ligand binding on the non-optimal side, and have a negative effect on the inhibitory activity of Aldose Reductase (AR) inhibitors. As such, it was recommended that the contour map be used as a guide to develop substituents that can be introduced in the light green favorable regions to improve protein-ligand interactions, and the large nonpolar groups were avoided in the red unfavorable regions to reduce steric hindrance.

3.4.1.3. Electron-Withdrawing Features

The electron-withdrawing (EWG) contour map obtained from the atom-based 3D-QSAR model shows the space around the molecule in which electron-withdrawing groups contribute to enhancing the aldose reductase (AR) inhibitory activity of the designed 1,3,4-thiadiazole derivatives. The maroon cube represents the favorable (positive) regions in the present atom-based 3D-QSAR contour map and suggests that placing an electron-withdrawing group (-F, -Cl, -Br, $-CF_3$, -CN, $-NO_2$, or a carbonyl-containing group) at these positions will increase inhibitory activity. Large contour areas of maroon color were seen around the

terminal alkyl side chain, the amino linker attached to the thiadiazole ring, the central fused heterocyclic region, and the terminal aromatic ring, all of which indicate that these positions were good for electron-withdrawing substitutions. These groups can increase the electronic distribution of the molecule, further strengthen protein-ligand interactions, and improve the stability of the ligand in the active site of aldose reductase, which consequently improves the binding affinity and inhibitory potencies. Favorable (positive) regions were represented by white cubes, whereas unfavorable (negative) regions were represented by blue cubes, and electron-withdrawing substituents in unfavorable regions can affect the biological activity. The present model indicates that the strong electron-withdrawing groups present at these positions could disrupt the optimal electronic environment, reduce the favorable interactions with active site residues, and disrupt the correct orientation of the ligand in the binding pocket. Hence, electron-withdrawing groups were preferred to be introduced in maroon favorable regions, and also the introduction of electron-withdrawing groups was not preferred in blue unfavorable regions to enhance the aldose reductase inhibitory activity (Figure 10C).

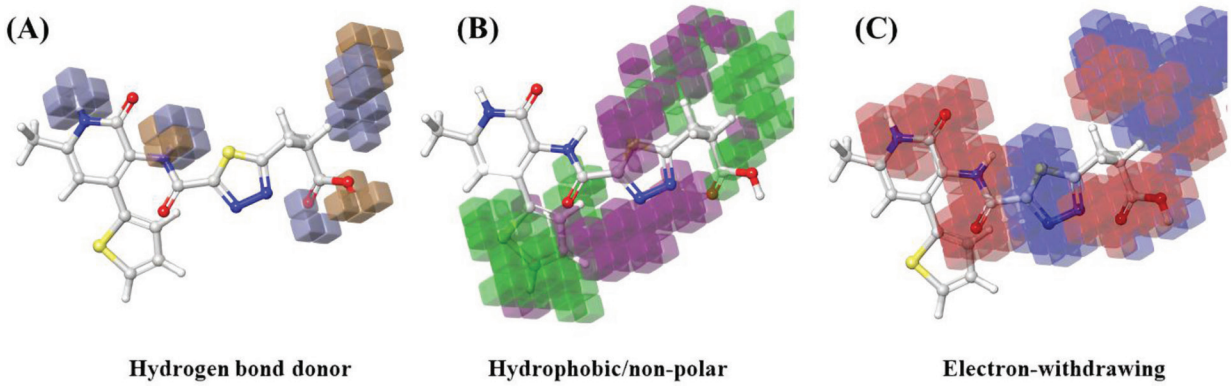

Figure 10: Atom-Based 3D-QSAR Models Colouring Representation of (A) Hydrogen Bond Donor; (B) Hydrophobic/Non-Polar; (C) Electron Withdrawing

Table 6: Data Set Analysis of Atom-Based QSAR Model

Factors	SD	R^2	R^2 CV	R^2 Scramble	Stability	F	P	RMSE	Q^2	Pearson-r
1	0.2127	0.5974	0.5576	0.5751	0.768	105.4	0.0296	0.25	0.5317	0.8351
2	0.2096	0.5561	0.5878	0.6079	0.652	113.6	0.0445	0.24	0.5175	0.6674
3	0.1463	0.6553	0.7213	0.7493	0.719	124.7	7.32e-05	0.21	0.6142	0.5139
4	0.1296	0.7428	0.7981	0.8634	0.855	143.7	8.01e-05	0.16	0.7137	0.8843

Table 7: Atom-Type Fraction 3D-QSAR Statistics

Factors	H-Bond Donor	Hydrophobic/Non-Polar	Electron-Withdrawing
1	0.023	0.685	0.225
2	0.036	0.722	0.205
3	0.061	0.789	0.136
4	0.066	0.782	0.143

3.5. Molecular Docking Analysis

Molecular docking with the catalytic binding pocket of Aldose Reductase (AR) was performed to assess the binding affinity and interaction profile of the selected compounds (04, 01, 02, 10, and 11) with AR as compared to the reference compound epalrestat (Figure 11). The highest binding affinity with a docking score of -10.178 kcal/mol was obtained with compound 04, which showed hydrogen-bond interaction with Gln183, His110, Trp111, and

Ala299; π-π stacking with Tyr209; π-cation interaction with Trp219; and a large number of hydrophobic interactions with Trp79, Ile260, Trp20, Val47, Tyr48, Phe122, Pro218, Val297, Cys298, Leu300, and Leu301, which led to a very stable binding conformation. Compound 01 had a docking score of -10.081 kcal/mol and formed hydrogen bonds with Asn160, Gln183, Cys298, and the carbonyl oxygen of the ligand; π-π stacking interactions with Trp20, Tyr209, and His110; a halogen bond with Ser302; and hydrophobic interactions with Trp79, Val47, Tyr48, Phe122, Pro218, Trp219, Ala299, Leu300, Leu301, and Cys298. Compound 02 demonstrated a docking score of -10.050 kcal/mol, forming hydrogen bonds with His110, Trp111, Gln183, Leu300, Leu301, and Ala299; π-π stacking with Tyr209; π-cation interaction with Trp219; and hydrophobic contacts with Trp79, Ile260, Trp20, Val47, Tyr48, Phe122, Pro218, Val297, Cys298, Leu300, and Leu301. Compound 10 had a docking score of -9.977 kcal/mol; it forms hydrogen bonds with Ser210, Gln183, His110, and Trp111; π-π stacking interactions with Tyr209; π-cation interaction with Trp219; and hydrophobic interactions with Trp79, Ile260, Trp20, Thr19, Val47, Tyr48, Phe122, Val297, Cys298, Pro218, Leu300, and Leu301. The compound 11 gave a docking score of –9.672 kcal/mol, forming hydrogen bonds with His110 and Gln183, π–π stacking with Tyr209 and Trp20 and hydrophobic interactions with Trp79, Trp111, Ile260, Thr19, Gly18, Val47, Tyr48, Pro218, Trp219, Cys298, Ala299, Leu300, and Leu301. Overall, all the selected compounds had some conserved interactions with the catalytic residues such as His110, Trp111, Gln183, Tyr209, Trp20, Trp79, Trp219, Phe122, Cys298, Ala299, Leu300, and Leu301, which are important for the recognition and stabilization of the ligand in the active site of aldose reductase. Epalrestat had a lower docking score of -8.182 kcal/mol that involved hydrogen bonding with His110, Tyr48, and Cys298; π-π stacking with Phe122; and hydrophobic interactions with Trp79, Trp111, Trp20, Val47, Leu124, Leu300, Leu301, Trp219, Cys298, Cys303, and Ser302. The significantly higher docking scores and stronger interaction networks of the designed 1,3,4-thiadiazole derivative compounds 04, 01, 02, 10, and 11 compared with Epalrestat (-8.182 kcal/mol) indicate that these compounds have more binding affinity and may be good lead compounds for the development of active substances against aldose reductase (Figure 12) (Table 8).

Table 8: Docking Scores (DS) of Dataset Compounds, R-group Enumerated Compounds, and Acarbose (Reference Compound)

Name of Compounds	Structure	DS (xp) kcal\mol	Interaction with Amino Acid Residues
04	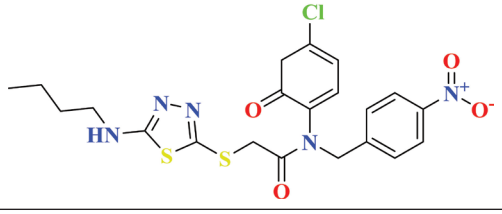	-10.178	TRP219 ALA299 LEU301 TRP111 HIE110 TYR209 GLN183
01	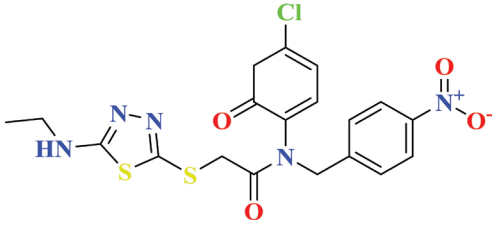	-10.081	TRP20 SER302 CYS298 HIE110 TYR209 GLN183 ASN160
02	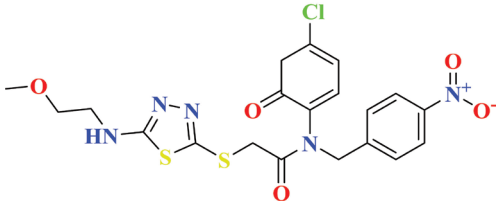	-10.050	HIE110 TRP111 LEU301 LEU300 ALA299 CYS298 TRP219 TYR209 GLN183

10	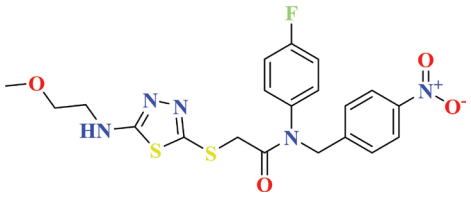	-9.977	LEU300 ALA299 CYS298 TRP219 TRP111 HIE110 GLN183 TYR209 SER210
11	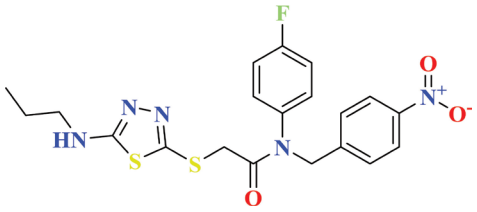	-9.672	TRP20 TYR209 GLN183 HIE110
PD01	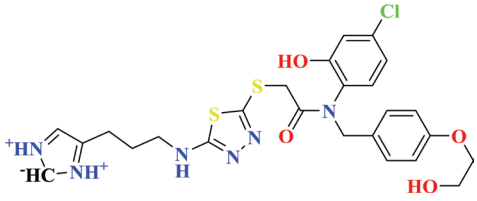	-10.605	HIE110 TRP111 TRP219 LEU300 VAL297 ARG296
Epalrestat	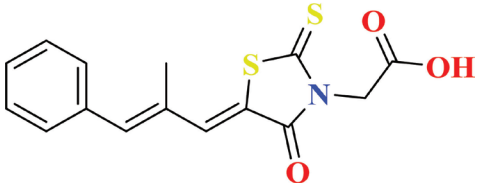	-8.182	HIE110 CYS298 TYR48 PHE122

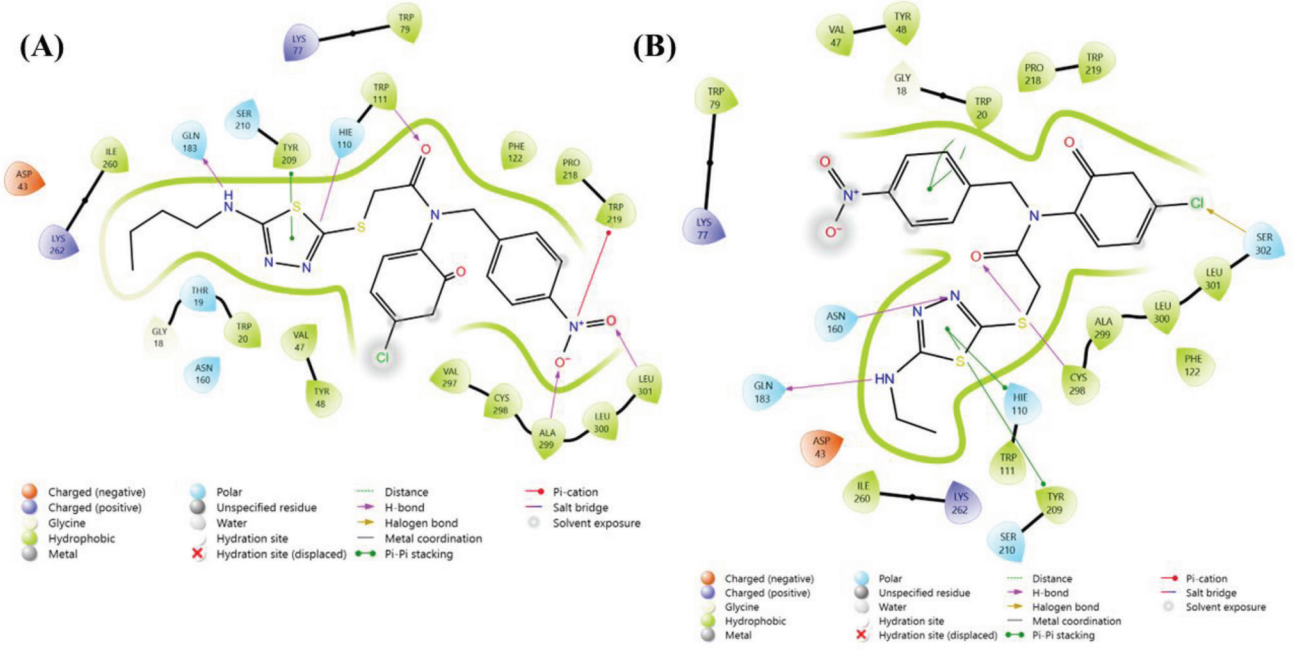

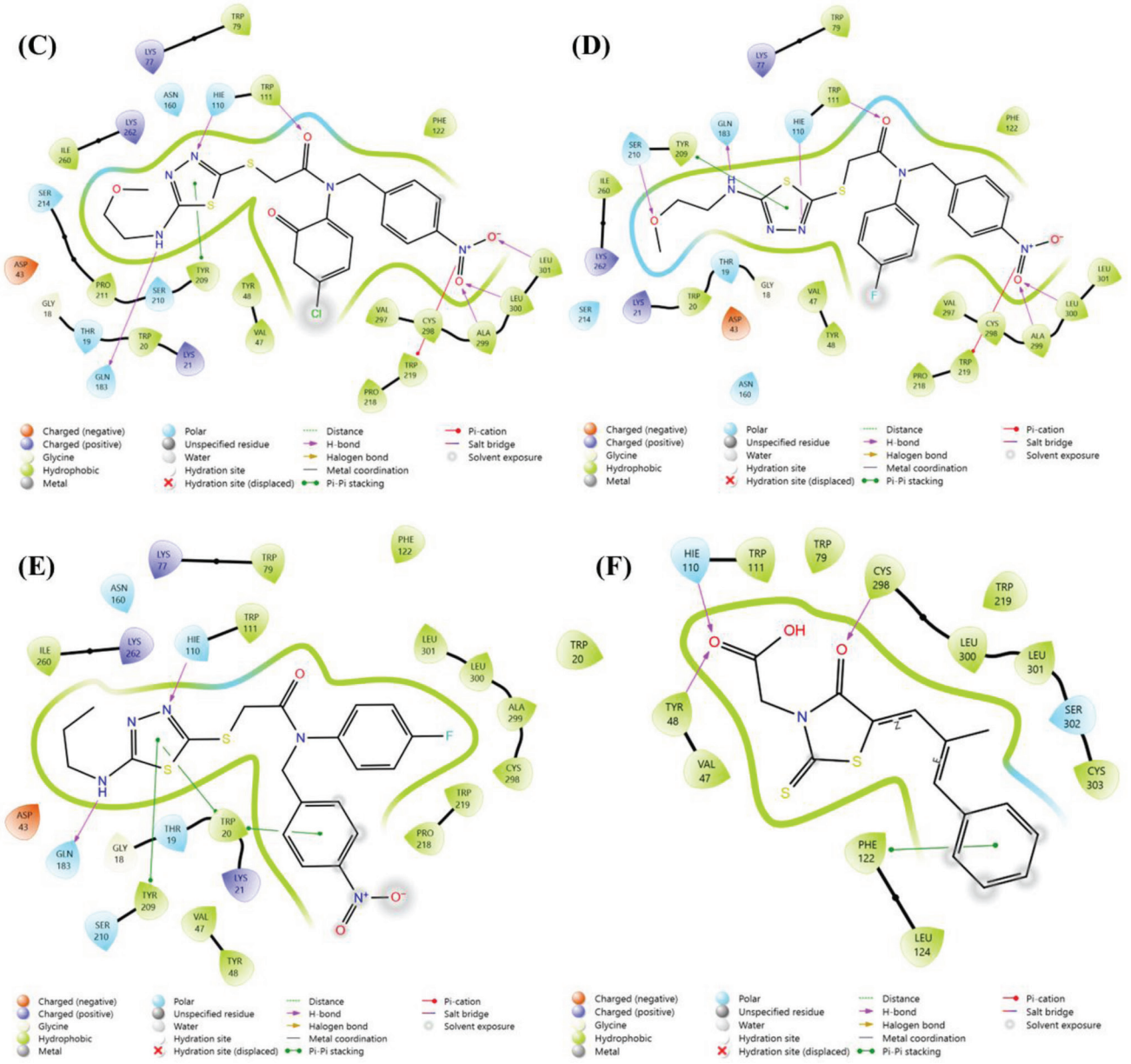

Figure 11: 2D Interactions of Data Set Compounds with Aldose Reductase (PDB ID: 4JIR) (A) Compound 4, (B) Compound 1, (C) Compound 2, (D) Compound 10, (E) Compound 11, (F) Epalrestat (Reference)

3.6. Virtual Screening Results of R-group-Enumerated Compounds

Using a strategy of electron withdrawal and diversity of hydrophobic groups, a virtual library of 1,419 novel 1,3,4-thiadiazole derivatives was created. The library was then virtually screened using a hierarchical approach in Schrödinger Maestro version 12.5. The High-Throughput Virtual Screening (HTVS) protocol was used to screen all the compounds. The molecules in the top 50% of the HTVS-ranked molecules were then re-docked with the Standard Precision (SP) protocol, and the top 20% of the hits from SP were re-docked using the Extra Precision (XP) protocol. Finally, the top 10% of XP-docked compounds were selected for detailed analysis, yielding optimized lead candidates. Of these 14 compounds, PD01 had a very good docking score of -10.605 kcal/mol, which was significantly better than the reference inhibitor Epalrestat (-8.182 kcal/mol). The carbonyl oxygen of the ligand formed hydrogen-bond interactions with His110, Trp219,

Val297, and Arg296, which play an important role in the stabilization of the protein-ligand complex. Additionally, π–π stacking interactions were seen with both Trp111 and Trp219 and also with the chlorophenyl ring, further stabilizing the binding within the catalytic pocket. A lot of hydrophobic interactions were also formed with Trp79, Trp111, Tyr48, Val47, Phe122, Ala299, Leu300, Leu301, Cys298, Trp295, Tyr209, Trp20, Ser302, and Asn294, making the binding orientation very stable. Epalrestat, the reference inhibitor, on the other hand, showed a docking score of -8.182 kcal/mol, with hydrogen-bond interactions with His110, Tyr48, and Cys298; π-π stacking with Phe122; and hydrophobic interactions with Trp20, Trp79, Trp111, Val47, Leu124, Leu300, Leu301, Trp219, Cys298, Cys303, and Ser302.

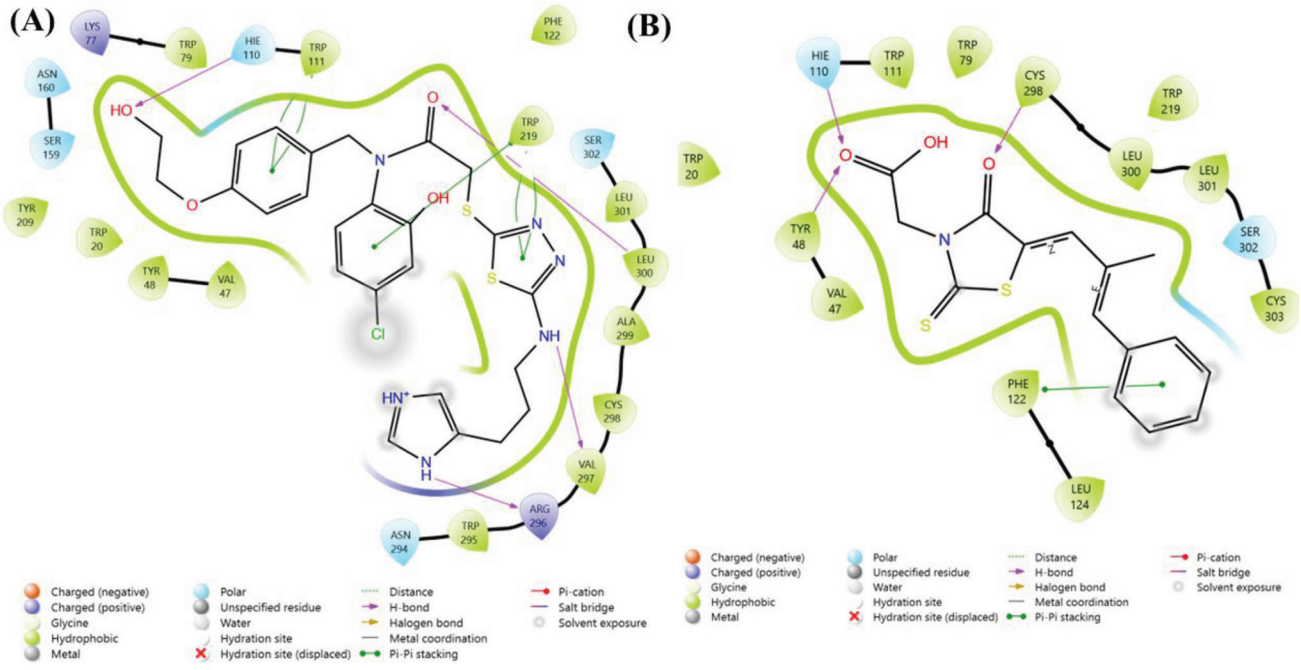

Figure 12: 2D Interactions of R-group Compounds (Designed) with Aldose reductase (PDB ID: 4JIR)- (A) Compound PD01, (B) Epalrestat (Reference)

3.7. Prediction of ADME Properties

The R-group-designed compound (PD01), the selected dataset compounds (04, 01, 02, 10, and 11), and the reference drug Epalrestat showed reasonable drug-likeness and oral drug development potential based on ADME properties predicted using the QikProp module in Schrödinger Maestro 12.5. Epalrestat had the lowest molecular weight (319.39 g/mol) and solvent-accessible surface area (566.82 Å²); had one hydrogen bond donor, 4.5 hydrogen bond acceptors, and moderate lipophilicity (QPlogPo/w = 3.602); and had excellent aqueous solubility (QPlogS = -3.322). These values show that it did not violate Lipinski's Rule of Five, and the predicted human oral absorption was high (84.51%). The selected compounds have moderate molecular size, with molecular weight ranging from 461.52 to 580.00 g/mol and solvent-accessible surface area ranging from 754.32 to 812.62 Å². All compounds had one hydrogen bond donor and hydrogen bond acceptors from 6.5 to 10.2, thus giving them good hydrogen bonding capability for target binding. The compounds had moderate lipophilicity (QPlogPo/w = 2.81-4.26) and adequate aqueous solubility (QPlogS = -5.45 to -7.34). The Caco-2 permeability values ranged from 66.38 to 143.54 nm/s, and MDCK permeability values ranged from 94.42 to 233.03 nm/s, indicating good membrane permeability. The QPlogBB values (-1.93 to -2.69) were indicative of limited penetration into the blood-brain barrier, desirable for those aldose reductase inhibitors targeted to the periphery, and the QPlogKhsa values (-0.55 to 0.35) were indicative of acceptable plasma protein binding. The predicted human oral absorption ranged from 64.89% (compound 02) to 90.26% (compound 11), with compound 11 showing the highest oral absorption, followed by compound 10 (87.05%), Epalrestat (84.51%),

compound 01 (76.03%), PD01 (75.68%), compound 04 (70.35%), and compound 02 (64.89%). The selected compounds were found to have good drug-likeness, with most of them having no or only one violation of Lipinski's Rule of Five, while PD01 had two violations of Lipinski's Rule of Five and two violations of Lipinski's Rule of Three, primarily because of the relatively high hydrogen-bond acceptor count and the molecular weight. However, PD01 exhibited good membrane permeability (Caco-2 = 99.75 nm/s; MDCK = 233.03 nm/s) and moderately good predicted oral absorption (75.68%). The overall results indicated that 1,3,4-thiadiazole derivatives, in general and especially compounds 10, 11, and PD01, exhibited balanced physicochemical properties, improved permeability, acceptable oral absorption, and good drug-like parameters, which made them promising candidates for further development as aldose reductase inhibitors (Table 9).

Table 9: ADME Properties of Dataset Compounds, R-group Enumerated Compounds, and Reference Compound Epalrestat

molecule	mol_MW	SASA	donorHB	accptHB	QPlog-Po/w	QPlog-HERG	QPP-Caco	Q-Plog-BB	QPPM-DCK	Q-Plog-Kp	QPlog-Khsa	Human Oral Absorption	Percent Human Oral Absorption	Rule Of Five	Rule Of Three
04	508.009	801.262	1	8.5	3.85	-6.069	77.589	-2.312	128.954	-3.938	0.347	1	70.351	1	1
01	479.955	707.667	1	8.5	2.813	-5.45	66.378	-2.06	94.423	-4.257	0.044	3	76.027	0	0
02	509.981	785.348	1	10.2	2.901	-6	78.498	-2.299	116.294	-3.923	-0.092	2	64.89	1	0
10	477.527	764.795	1	8.2	3.671	-6.276	143.539	-2.024	171.696	-3.166	0.212	3	87.048	0	0
11	461.528	750.432	1	6.5	4.257	-6.192	139.621	-1.933	182.646	-3.289	0.545	1	90.263	0	1
Epalrestat	319.393	566.82	1	4.5	3.602	-3.322	109.132	-0.946	172.932	-2.868	-0.016	3	84.512	0	0
PD01	575.099	924.795	4	10.2	4.426	-7.335	99.75	-2.659	233.025	-2.742	0.268	1	75.677	2	2

Representation of: (QPlog Po/w) Octanol/water partition coefficient; (QPPCaco) cell permeability (nm/s); (QPlogBB) Brain/blood partition coefficient (QPPMDCK) Apparent MDCK cell permeability (nm/s) (SASA) Solvent-accessible surface area; Human serum albumin binding: 6 per cent human oral absorption.

4. Optimisation of Novel Ligands

The 3D-QSAR contour maps, along with the AHHRR_1 pharmacophore model, proved to be useful for understanding the structure-activity relationship (SAR) of the 1,3,4-thiadiazole derivatives and identified the structural features that contribute to their inhibitory activity against aldose reductase. The SAR analysis indicated that the hydrophobic groups like phenyl, substituted phenyl, benzyl, alkyl, cycloalkyl, and heteroaromatic groups at the desirable substitution points markedly improved the inhibitory activity by increasing the hydrophobic and π-π interactions in the binding pocket of aldose reductase. Appropriate hydrogen bond donor groups at the wrong locations, however, caused a decrease in the inhibitory activity, which was likely due to steric hindrance and the orientation of the ligand inside the active site. Further, the contour map analysis suggested that the introduction of those groups that are electron-withdrawing, such as -F, -Cl, -Br, $-CF_3$, -CN, $-NO_2$, carbonyl groups and sulfonyl groups at the favourable positions, enhanced the inhibitory activity by improving the electronic properties of the molecules and facilitating stronger interactions with key catalytic residues. However, the addition of electron-donating groups ($-CH_3$, $-OCH_3$, and $-NH_2$) and too many substitutions at an unfavourable position were expected to reduce biological activity because of disruption of favourable protein-ligand interactions. From the overall result of the combined AHHRR_1 pharmacophore model and atom-based 3D-QSAR analysis, it could be concluded that the strategic attachment of hydrophobic substituents along with appropriate electron-withdrawing groups at the favourable contour regions was one of the effective ways for the rational design and optimisation of more potent 1,3,4-thiadiazole-based aldose reductase inhibitors (Figure 13).

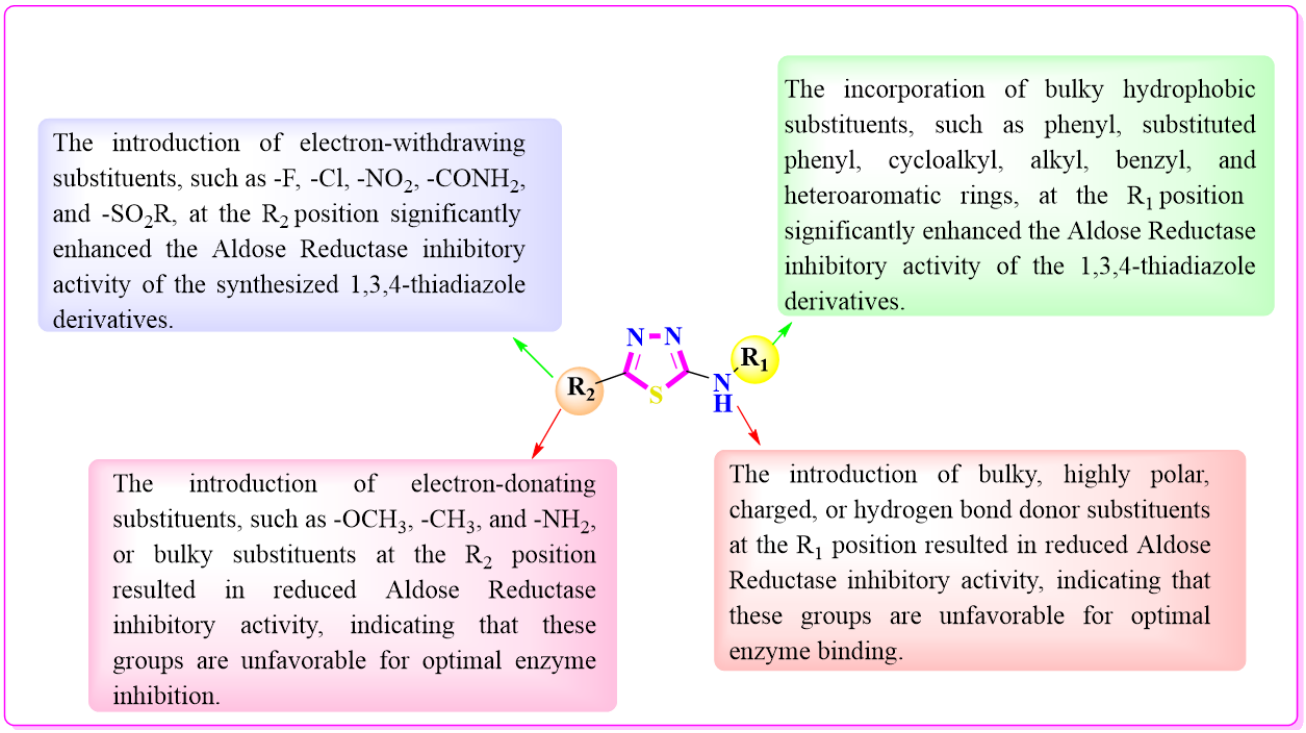

Figure 13: SAR of 1,3,4-Thiadiazole Moiety as Aldose Reductase Inhibitory Activity

5. Conclusion

The present study identified the 1,3,4-thiadiazole scaffold as a promising template for the development of novel aldose reductase inhibitors. The pharmacophore and validated atom-based 3D-QSAR analyses revealed that hydrophobic substituents and appropriately positioned electron-withdrawing groups are the key structural features associated with enhanced inhibitory activity, providing useful guidelines for the rational optimization of this scaffold. Molecular docking studies demonstrated that several compounds showed strong binding within the catalytic pocket of aldose reductase and better predicted binding affinity than the standard inhibitor Epalrestat. Among all the compounds evaluated, the designed derivative PD01 emerged as the most promising lead candidate, exhibiting the highest docking score and favorable interactions with the conserved catalytic residues of the enzyme. In addition, PD01 showed acceptable physicochemical properties, drug-likeness, membrane permeability, and predicted oral absorption, indicating its potential suitability as an orally active drug candidate. Overall, this study provides valuable structural insights into aldose reductase inhibition and supports the use of integrated computational strategies for the rational design of safer and more effective next-generation aldose reductase inhibitors for the management of diabetes-associated complications.

Abbreviations

3D-QSAR: Three-Dimensional Quantitative Structure-Activity Relationship; **DM:** Diabetes Mellitus; **HBA:** Hydrogen Bond Acceptor; **HBD:** Hydrogen Bond Donor; **LOO:** Leave-One-Out; **PLS:** Partial Least Square; **RMSD:** Root Mean Square Deviation; **SASA:** Solvent Accessible Surface Area; **SD:** Standard Deviation; T2DM: Type 2 Diabetes Mellitus; **HTVS:** high-throughput virtual screening; **PDB:** Protein Data Bank; **XP:** extra precision; **ADME:** absorption, distribution, metabolism and excretion; **EWGs:** electron-withdrawing groups

Acknowledgement

The authors sincerely acknowledge the Department of Pharmaceutical Chemistry, SWIFT School of Pharmacy, Rajpura, Punjab, India, and the University School of Pharmaceutical Sciences, Rayat Bahra University, Hoshiarpur, Punjab, India, for providing the academic environment and research facilities necessary for this study. The authors gratefully acknowledge Schrödinger, LLC, New York, NY, USA, for providing access to the Schrödinger Suite under the academic licensing program used in this study. Finally, the authors thank their colleagues and mentors for their valuable discussions and continuous support throughout this research.

Authorship Contribution

Debarshi Mondal conceptualized the present research work and interpreted the molecular docking and 3D-QSAR results. Priya Devi performed the molecular docking study, wrote the original draft and performed 3D-QSAR studies. Shalini Sharma and Dr. Harmel Singh Chahal checked the final draft of the manuscript.

Funding

This research did not receive any specific grant from funding agencies in the public, commercial, or not-for-profit sectors.

Conflict of Interest

The authors declare no conflict of interest related to this study.

Declarations

The authors declare that this work is original and has not been submitted elsewhere for publication. All data, methodologies, and system components have been developed and reported in adherence to academic standards. All referenced materials have been duly cited, and the authors accept full responsibility for the integrity and accuracy of the findings presented.

Ethical Approval

Ethical approval was not required for this study as it involved only computational and in silico analyses and did not involve human participants, animals, or biological samples.

Human and Animal Rights

No humans or animals were involved in this research.

Data Availability Statement

The authors confirm that the data supporting the conclusions of this study are included within the article.

Figure Permissions

All figures included in this manuscript are original, created by the authors, and don't require permission from any third party. The authors retain the rights to these figures and grant the publisher permission to reproduce them as part of this publication.

AI Disclosure Statement

The authors declare that artificial intelligence (AI) assisted tools were used solely for language enhancement, grammar checking, and improving the readability of the manuscript.

References

Acar Çevik, U., Celik, I., Işık, A., Ahmad, I., Patel, H., Özkay, Y., & Kaplancıklı, Z. A. (2023). Design, synthesis, molecular modeling, DFT, ADME and biological evaluation studies of some new 1,3,4-oxadiazole linked benzimidazoles as anticancer agents and aromatase inhibitors. *Journal of Biomolecular Structure and Dynamics, 41*(5), 1944–1958. https://doi.org/10.1080/07391102.2022.2025906

Ahmed, S. S., & Rahman, M. O. (2024). From flora to pharmaceuticals: 100 new additions to angiosperms of Gafargaon subdistrict in Bangladesh and unraveling antidiabetic drug candidates targeting DPP4 through *in silico* approach. *PLOS ONE, 19*(3), e0301348. https://doi.org/10.1371/journal.pone.0301348

Akdağ, M., Çam, M. G., Ergen, D., Demir, Y., Beydemir, Ş., & Özçelik, A. B. (2025). Synthesis of new pyridazinone derivatives and their dual inhibitory activity on aldose reductase and α-glucosidase. *Bioorganic & Medicinal Chemistry Letters*, 130498. https://doi.org/10.1016/j.bmcl.2025.130498

Asati, V., Bharti, S. K., & Budhwani, A. K. (2017). 3D-QSAR and virtual screening studies of thiazolidine-2,4-dione analogs: Validation of experimental inhibitory potencies towards PIM-1 kinase. *Journal of Molecular Structure, 1133*, 278–293. https://doi.org/10.1016/j.molstruc.2016.12.006

Balestri, F., Moschini, R., Mura, U., Cappiello, M., & Del Corso, A. (2022). In search of differential inhibitors of aldose reductase. *Biomolecules, 12*(4), 485. https://doi.org/10.3390/biom12040485

Bisht, P., Gautam, P., Bhattacharya, A., Singh, R., & Verma, S. K. (2025). Designing of xanthine-based DPP-4 inhibitors: A structure-guided alignment dependent multifacet 3D-QSAR modeling, and molecular dynamics simulation study. *Journal of Biomolecular Structure and Dynamics, 43*(13), 6971–6995. https://doi.org/10.1080/07391102.2024.2329787

Brownlee, M. (2001). Biochemistry and molecular cell biology of diabetic complications. *Nature, 414*(6865), 813–820. https://doi.org/10.1038/414813a

Chung, S. S. M., & Chung, S. K. (2005). Aldose reductase in diabetic microvascular complications. *Current Drug Targets, 6*(4), 475–486. https://doi.org/10.2174/1389450054021891

Gholami Rostami, E., & Fatemi, M. H. (2018). Comparative molecular field analysis and hologram quantitative structure activity relationship studies of pyrimidine series as potent phosphodiesterase 10A inhibitors. *Journal of the Chinese Chemical Society, 65*(11), 1293–1306. https://doi.org/10.1002/jccs.201700435

Gholami Rostami, E., & Fatemi, M. H. (2019). Molecular docking and receptor-based QASR studies on pyrimidine derivatives as potential phosphodiesterase 10A inhibitors. *Structural Chemistry, 30*(6), 2347–2368. https://doi.org/10.1007/s11224-019-01353-6

Gupta, S., Saha, M., Singh, R., Ahmed, S. B., & Asati, V. (2025). Multistage *in silico* approach to identify novel quinoline derivatives as potential c-kit kinase inhibitors. *Journal of Biomolecular Structure and Dynamics, 43*(11), 5313–5330. https://doi.org/10.1080/07391102.2024.2308759

Haritha, M., Sreerag, M., & Suresh, C. H. (2024). Quantifying the hydrogen-bond propensity of drugs and its relationship with Lipinski's rule of five. *New Journal of Chemistry, 48*(11), 4896–4908. https://doi.org/10.1039/D3NJ05476D

Hosen, S. Z., Dash, R., Khatun, M., Akter, R., Bhuiyan, M. H. R., Karim, M. R., ... & Afrin, S. (2017). *In silico* ADME/T and 3D QSAR analysis of KDR inhibitors. *Journal of Applied Pharmaceutical Science, 7*(1), 120–128. https://doi.org/10.7324/JAPS.2017.70116

Inamdar, A., Pote, S., Sawant, S., Salve, P. S., Suryawanshi, S. S., & Palled, M. (2023). Physicochemical and pharmacokinetic properties' screening of selected cardiovascular agents: An *in silico* approach. https://doi.org/10.21203/rs.3.rs-2653667/v1

Kaya, B., Acar Çevik, U., Çiftçi, B., Duran, H. E., Türkeş, C., Işık, M., ... & Beydemir, S. (2024). Synthesis, α-glucosidase, α-amylase, and aldose reductase inhibitory activity with molecular docking study of novel imidazo[1,2-a]pyridine derivatives. *ACS Omega, 9*(42), 42905–42914. https://doi.org/10.1021/acsomega.4c05619

Kaya, B., Acar Çevik, U., Necip, A., Duran, H. E., Çiftçi, B., Işık, M., ... & Beydemir, S. (2025). Design, synthesis, biological evaluation, and molecular docking studies of novel 1,3,4-thiadiazole derivatives targeting both aldose reductase and aldose reductase for diabetes mellitus. *ACS Omega, 10*(18), 18812–18828. https://doi.org/10.1021/acsomega.5c00566

Oates, P. J. (2008). Aldose reductase, still a compelling target for diabetic neuropathy. *Current Drug Targets, 9*(1), 14–36.

Oates, P. J., & Mylari, B. L. (1999). Aldose reductase inhibitors: Therapeutic implications for diabetic complications. *Expert Opinion on Investigational Drugs, 8*(12), 2095–2119. https://doi.org/10.1517/13543784.8.12.2095

Polya, G., & Read, R. C. (2012). *Combinatorial enumeration of groups, graphs, and chemical compounds*. Springer Science & Business Media. https://doi.org/10.1007/978-1-4612-4664-0

Ramunno, A., Cosconati, S., Sartini, S., Maglio, V., Angiuoli, S., La Pietra, V., ... & Novellino, E. (2012). Progresses in the pursuit of aldose reductase inhibitors: The structure-based lead optimization step. *European Journal of Medicinal Chemistry, 51*, 216–226. https://doi.org/10.1016/j.ejmech.2012.02.045

Sharma, R., Roy, S., & Kumar, A. (2025). Drug repurposing and virtual screening. In K. Jain & A. K. Yadav (Eds.), *Advances in pharmaceutical product development*. Springer. https://doi.org/10.1007/978-981-97-9230-6_16

Shulgau, Z., Palamarchuk, I. V., Sergazy, S., Urazbayeva, A., Ramankulov, Y., & Kulakov, I. V. (2024). Synthesis, computational study, and *in vitro* aldose reductase inhibitory action of 1,3,4-thiadiazole derivatives of 3-aminopyridin-2(1H)-ones. *Pharmaceuticals, 17*(3), 377. https://doi.org/10.3390/ph17030377

Singh Grewal, A., Bhardwaj, S., Pandita, D., Lather, V., & Singh Sekhon, B. (2016). Updates on aldose reductase inhibitors for management of diabetic complications and non-diabetic diseases. *Mini Reviews in Medicinal Chemistry, 16*(2), 120–162. https://doi.org/10.2174/1389557515666150909143737

Singh, Y., Jaswal, S., Singh, S., Verma, S. K., & Thareja, S. (2022). Dual aromatase-steroid sulfatase inhibitors (DASI's) for the treatment of breast cancer: A structure guided ligand based designing approach. *Journal of Biomolecular Structure and Dynamics, 41*(20), 10604–10626. https://doi.org/10.1080/07391102.2022.2155702

Srivastava, S. K., Ramana, K. V., & Bhatnagar, A. (2005). Role of aldose reductase and oxidative damage in diabetes and the consequent potential for therapeutic options. *Endocrine Reviews, 26*(3), 380–392. https://doi.org/10.1210/er.2004-0028

Stitou, M., Toufik, H., Bouachrine, M., & Lamchouri, F. (2021). Quantitative structure–activity relationships analysis, homology modeling, docking and molecular dynamics studies of triterpenoid saponins as Kirsten rat sarcoma inhibitors. *Journal of Biomolecular Structure and Dynamics, 39*(1), 152–170. https://doi.org/10.1080/07391102.2019.1707122

Vanajothi, R., Hemamalini, V., Jeyakanthan, J., & Premkumar, K. (2020). Ligand-based pharmacophore mapping and virtual screening for identification of potential discoidin domain receptor 1 inhibitors. *Journal of Biomolecular Structure and Dynamics, 38*(9), 2800–2808. https://doi.org/10.1080/07391102.2019.1640132

Veerasamy, R., Rajak, H., Jain, A., Sivadasan, S., Varghese, C. P., & Agrawal, R. K. (2011). Validation of QSAR models-strategies and importance. *International Journal of Drug Design and Discovery, 3*, 511–519. https://doi.org/10.37285/ijddd.2.3.1

Verma, S. K., Kumar, N., & Thareja, S. (2021). Gaussian field-based comparative 3D QSAR modelling for the identification of favourable pharmacophoric features of chromene derivatives as selective inhibitors of ALR2 over ALR1. *Structural Chemistry, 32*(3), 1289–1298. https://doi.org/10.1007/s11224-020-01714-6

Vishwakarma, K., & Bhatt, H. (2021). Molecular modelling of quinoline derivatives as telomerase inhibitors through 3D-QSAR, molecular dynamics simulation, and molecular docking techniques. *Journal of Molecular Modeling, 27*(2), 30. https://doi.org/10.1007/s00894-020-04648-2

Yadav, R., Imran, M., Dhamija, P., Chaurasia, D. K., & Handu, S. (2021). Virtual screening, ADMET prediction and dynamics simulation of potential compounds targeting the main protease of SARS-CoV-2. *Journal of Biomolecular Structure and Dynamics, 39*(17), 6617–6632. https://doi.org/10.1080/07391102.2020.1796812